# PARAMETER IDENTIFICATION OF A SPACE OBJECT IN THE PRE-CAPTURE PHASE

Olga-Orsalia Christidi-Loumpasefski and Evangelos Papadopoulos

*National Technical University of Athens*
*School of Mechanical Engineering - Control Systems Laboratory*
*9 Heroon Polytechneiou Str., 15780, Athens, Greece Country,*
*E-mail: {olgaloumpasefski@gmail.com, egpapado@central.ntua.gr}*

## ABSTRACT

A method for identifying the full set of inertial parameters of a space object on orbit is presented, which is applicable at the pre-capture phase. The method's objective is to reduce the risk during the capture phase, the most critical of a mission. Using data from visual and force sensors, the object's center of mass, mass and moments of inertia are estimated. No information about accelerations, which contain substantial noise, is required. The proposed method is validated by a numerical simulation and followed by the experimental identification of a floating passive object, part of the NTUA Space Emulator System.

## 1 INTRODUCTION

On-orbit Servicing is a continuously growing area that concerns space programs all over the world. Therefore, research in this area is of vital importance. A high number of satellites are placed on-orbit over the past 50 years, resulting in a large number of space debris that endanger the success of current and future missions.

On-orbit Servicing includes missions, such as re-orbiting and de-orbiting, inspection and retrofitting of orbiting structures, satellite maintenance, satellite repair, and removal of space debris. In the past two decades, many technologies and methods have been developed and several on-orbit experimental missions have been completed. These missions were using cooperative target satellites; however, many satellites on orbit, have become uncooperative. In this case, one of the greatest challenges is to ensure the successful docking between the chaser satellite and the target system, or the safe and reliable capture of the target to stabilize it for subsequent servicing, [1]. These tasks can benefit substantially from the accurate knowledge of target parameters, since the high precision required can only be achieved by the implementation of advanced model based control strategies. Therefore, the need for parameter identification methods arises.

After having completed the far and close-range rendezvous maneuvers, with the target satellite, the servicing spacecraft remains at a safe, station-keeping distance from the tumbling target satellite.

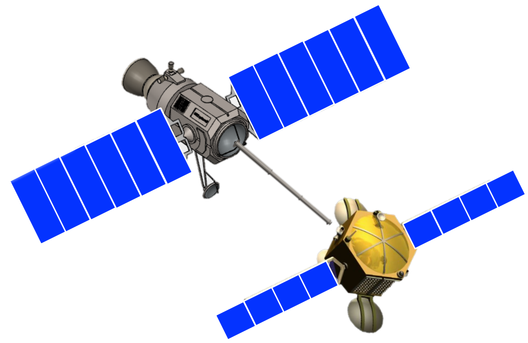

*Figure 1: A chaser satellite deploys a rod in order to touch the space object in pre-capture phase*

Then, the capture operation mode can start. To identify the target satellite parameters, some researchers have proposed methods that require the capture phase to be accomplished first, while others proposed methods that can be applied during the pre-capture phase. Some of the methods that require the capture phase to be accomplished before the identification procedure, identify the chaser's base body, the end-effector payload, or the target satellite, [2], [3], while others obtain full knowledge of the combined system, [4], [5].

However, to reduce risks during the capture procedure, it is vital to identify fully a target's inertia parameters during the pre-capture phase. The proposed methods that can be applied in this case are mainly vision-based, [6], [7], [8]. These methods can estimate only the ratios of the moments of inertia, the location of the center of mass (CoM) and the orientation of the principal axes. However, to accomplish highly complicated tasks, full knowledge of the model is required, not some of its parameters only.

To compensate for this lack of knowledge, Sheinfeld and Rock [9], presented a two-step inertia estimation procedure. In the first step, the servicing satellite tracks the target, and estimates the same quantities with those estimated by the aforementioned vision-based methods. However, manipulation tasks also require knowledge of the total mass and of the moments and products of inertia scale factors. Hence, a second step is proposed, during which the servicing satellite applies forces and moments to the target (e.g. by making contact with a manipulator). To this end, it was proposed to employ an impulse to estimate the required parameters (scale factors and total mass); however, this step was not implemented [9]. Meng et al. [10] address this need by applying a number of impulses to the target object, and using an extended Kalman filter, least squares, and observation data from visual and force sensors, they estimate in simulations all target inertial parameters. Although this idea is similar to that proposed in this paper, in [10] no specific scenario is simulated, i.e. a specific way to apply the impulse, leading to unsolved related issues, i.e. the issue of how to calculate the forces applied on the target based on the forces measured by the force sensor mounted on the chaser remains open. In their simulations, the issue of estimating the location of impulse application is not considered while the noise of force sensor measurements is not considered either.

In this paper, a method for identifying the full set of inertial parameters of a space object is presented, which is applicable during the pre-capture phase. Using data from visual sensors, the object's CoM and the velocity of the CoM are estimated. An impulse is applied on the target object by a rod mounted on the chaser system, see Fig. 1. Using data provided by visual and force sensors mounted on the chaser system, the object's mass and moments of inertia are estimated. The method is based on kinematic and the impulse equation; no information about accelerations, which contain substantial noise, is required. The proposed method is validated by a numerical simulation and followed by the experimental identification of a floating passive object, part of the NTUA Space Emulator System.

## 2 IDENTIFICATION METHOD

The proposed identification method is developed for implementation during the pre-capture phase. Particularly, this phase will take place after the station-keeping phase and before the capture phase, and can be divided into five sub-phases. Firstly, the chaser satellite deploys a rigid rod. Secondly, the chaser observes the target motion and plans how to approach and touch the target. During the third phase the robot moves toward the planned location for the contact. The fourth phase consists of the actual impact phase in which the rigid rod physically touches the target satellite. In the final phase, the chaser moves backward to avoid an undesirable contact with the target that would prevent the capture phase. This method will focus on the observation of target motion and the actual impact phase, since the identification procedure will take place during these phases. Moreover, the proposed method is employing kinematics and impulse equations. By taking measurements before, after and during the impact from visual and force sensors, and by using least squares, the full knowledge of a target model is obtained, to become available to the control system for safe and reliable capture of the tumbling target.

### 2.1 Estimation of a target's CoM

In this procedure, it is assumed that there is a vision system mounted on the chaser satellite, which tracks the position of some feature points on the surface of the target object. In particular, at least four points have to be tracked, in order to represent the attitude of the tumbling object. Specifically in this work, the required measurements are the position and velocity of one feature point and the attitude and angular velocity of an observation frame (frame ***b***) attached to the target, see Fig. 2. The feature's velocity can be represented by the following kinematic equation,

$$\mathbf{v}_1 = \mathbf{v}_{cm} + \boldsymbol{\omega} \times \mathbf{r}_0 \qquad (1)$$

where $\mathbf{v}_1$ is the velocity of the feature, $\mathbf{v}_{cm}$ is the velocity of target's CoM, which remains constant when the space object is free-floating, $\boldsymbol{\omega}$ is the angular velocity of the object, and $\mathbf{r}_0$ is the vector from target's CoM to the feature point.

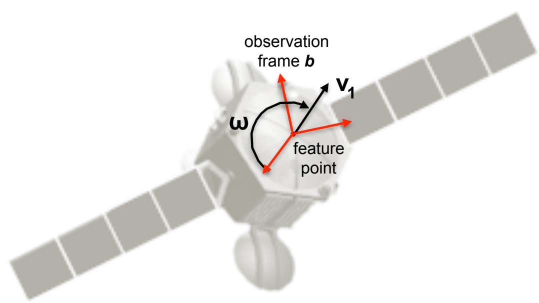


*Figure 2: Object's feature point and observation frame schematically.*

All quantities described are expressed in the inertial frame. To estimate the CoM location, (1) must contain a quantity about the CoM, which remains constant over time. Hence, the vector $\mathbf{r}_0$ must be expressed in the observation frame, i.e. as ${}^{b}\mathbf{r}_0$,

$$\mathbf{v}_1 = \mathbf{v}_{cm} + \boldsymbol{\omega}^{\times} \mathbf{R}_b \, {}^{b}\mathbf{r}_0 \qquad (2)$$

where $\mathbf{R}_b$ is the rotation matrix, which represents the relative attitude of object's observation frame with respect to the inertial frame, and $(\cdot)^{\times}$ stands for the cross product skew symmetric matrix of $(\cdot)$.

While the object is free-floating, $N$ measurements are used at time instants $t_1, t_2, \ldots, t_N$ of feature's position and object's attitude. The position is differentiated to obtain velocity. Without loss of generality, and assuming that the attitude is represented by the quaternion $\boldsymbol{\varepsilon}, \eta$, the angular velocity of the target is obtained by differentiating the quaternion and by solving for the angular velocity in the following equation, [11]

$$\begin{bmatrix} \dot{\boldsymbol{\varepsilon}} \\ \dot{\eta} \end{bmatrix} = \frac{1}{2}\mathbf{R}_b^{\mathrm{T}} \begin{bmatrix} \boldsymbol{\varepsilon}^{\times} + \eta \mathbf{I}_3 \\ -\boldsymbol{\varepsilon}^{\mathrm{T}} \end{bmatrix} \boldsymbol{\omega} \tag{3}$$

where $\mathbf{I}_3$ is the 3x3 identity matrix.

Hence, the following system of equations arose,

$$\begin{aligned} \mathbf{v}_{1|t_1} &= \mathbf{v}_{cm} + \boldsymbol{\omega}^{\times}_{|t_1} (\mathbf{R}_{b_{|t_1}} {}^{b}\mathbf{r}_0) \\ \mathbf{v}_{1|t_2} &= \mathbf{v}_{cm} + \boldsymbol{\omega}^{\times}_{|t_2} (\mathbf{R}_{b_{|t_2}} {}^{b}\mathbf{r}_0) \\ &\dots \\ \mathbf{v}_{1|t_N} &= \mathbf{v}_{cm} + \boldsymbol{\omega}^{\times}_{|t_N} (\mathbf{R}_{b_{|t_N}} {}^{b}\mathbf{r}_0) \end{aligned} \tag{4}$$

Equations (4) can be written in a matrix form as

$$\mathbf{A}\mathbf{x} = \mathbf{b} \tag{5}$$

where

$$\mathbf{A} = \begin{bmatrix} \mathbf{I}_3 & \boldsymbol{\omega}^{\times}_{|t_1} \mathbf{R}_{b_{|t_1}} \\ \mathbf{I}_3 & \boldsymbol{\omega}^{\times}_{|t_2} \mathbf{R}_{b_{|t_2}} \\ \dots & \dots \\ \mathbf{I}_3 & \boldsymbol{\omega}^{\times}_{|t_N} \mathbf{R}_{b_{|t_N}} \end{bmatrix}$$

$$\mathbf{x} = \begin{bmatrix} \mathbf{v}_{cm} \\ {}^{b}\mathbf{r}_0 \end{bmatrix} \tag{6}$$

$$\mathbf{b} = \begin{bmatrix} \mathbf{v}_{1|t_1} \\ \mathbf{v}_{1|t_2} \\ \dots \\ \mathbf{v}_{1|t_N} \end{bmatrix}$$

To solve for $\mathbf{x}$, see Fig. 3, at least two measurements are required. The system (5) is over-determined and is solved using least-squares as

$$\mathbf{x} = (\mathbf{A}^{\mathrm{T}}\mathbf{A})^{-1}\mathbf{A}^{\mathrm{T}}\mathbf{b} \tag{7}$$

Thus, object's CoM and its velocity can be estimated any time while the system is free-floating.

## 2.2 Estimation of the target's mass

In this procedure, it is assumed that there is a deployable rigid rod mounted on the chaser satellite, which can apply a small impulse to the space object, keeping the chaser satellite at a safe distance from the object. A force sensor is mounted either on the chaser body or on the rod tip. Estimation of the target mass can be divided in three sub-phases. Initially, the vision system tracks a feature point of the target, as discussed in Section 2.1. Solving (7), the velocity of the object CoM is identified. Then, the rod is deployed and the chaser system approaches the target. The rod touches slightly the

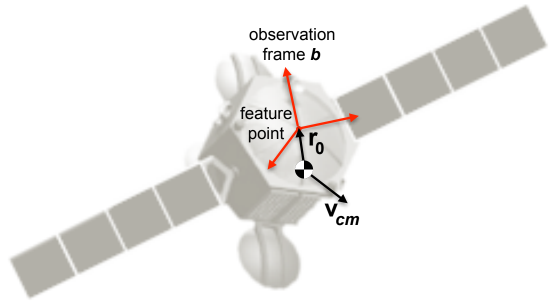


*Figure 3: Object's feature point and observation frame schematically.*

target and the force sensor mounted on the chaser system measures the interaction force. Also the duration of contact is measured. Hence, the impulse is calculated; the impulse that acts on the target is the opposite one. Finally, the vision system tracks again the feature point of the target and by solving (7) the velocity of object's CoM after the impulse application is estimated.

The estimation of the mass is based on momentum calculations, avoiding the highly noisy acceleration measurements, i.e.

$$M\mathbf{v}_{cm_{|t_1}} + \int_{t_1}^{t_2} \mathbf{F}_{contact} dt = M\mathbf{v}_{cm_{|t_2}} \tag{8}$$

where $M$ is object's mass and $\mathbf{F}_{contact}$ is the contact force applied on the target. The feature's velocity is constant before the application of the impulse by the rod and is represented in (8) as $\mathbf{v}_{cm_{|t_1}}$. Accordingly, the feature's velocity after the application of the impulse by the rod is represented as $\mathbf{v}_{cm_{|t_2}}$. Without loss of generality, the above equation can be written for a single axis, e.g. the y-axis, and solved for $M$,

$$M = \frac{\int_{t_1}^{t_2} F_{contact_y} dt}{v_{cm_{y|t_2}} - v_{cm_{y|t_1}}} \tag{9}$$

## 2.3 Estimation of target's moments of inertia

The identification procedure for target's moments of inertia takes place during the same sub-phases as these described in the previous section for mass estimation. In particular, the vision system initially tracks the observation frame attached to the target and the attitude of the target is obtained. Using (3) angular velocity is obtained.

Subsequently, the rod is deployed and the chaser system approaches the target. The rod touches slightly the target and the force sensor mounted on the chaser system measures the force acting on this. Also the time duration of contact is measured. To calculate the moment impulse acting on the object and assuming that the contact occurs at a point, the vector from the object's CoM to the point of the contact force application must be estimated. For this purpose, it is proposed to measure the position of the chaser system at the time of contact, i.e. $\boldsymbol{r}_{GPS}$, see Fig. 4. Furthermore, assuming the rod has a small diameter, the vector from the point on the chaser the GPS sensor is mounted to the end of the rod is already known from CAD model, i.e. $\boldsymbol{r}_{rod}$.

The tip of the rod coincides with the contact force application point on the chaser system. Hence, the vector from the object's CoM to the point of the contact force application, i.e. $\boldsymbol{r}_f$, can be calculated by the following equation

$$\mathbf{r}_f = \mathbf{r}_{GPS} + \mathbf{r}_{rod} - \mathbf{r}_{cm} \tag{10}$$

where

$$\mathbf{r}_{\mathbf{cm}} = \mathbf{r}_1 - \mathbf{R}_b\,{}^b\mathbf{r}_0 \tag{11}$$

where $\mathbf{r}_1$ is the object's feature position measured by the visual sensors and ${}^b\mathbf{r}_0$ is already identified visually, before the impulse application (see Section 2.1). Finally, the vision system tracks the attitude of the observation frame after the impulse.

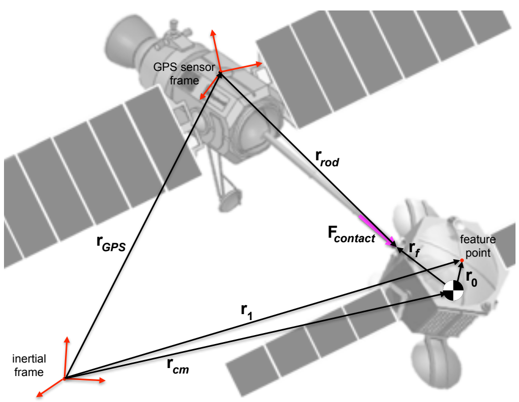


*Figure 4: Contact kinematics.*

The moment impulse theorem can be written as,

$$\mathbf{I}\boldsymbol{\omega}\big|_{t_{N_1}} + \int_{t_{N_1}}^{t_{N_2}} (\mathbf{r}_f \times \mathbf{F}_{contact})dt = \mathbf{I}\boldsymbol{\omega}\big|_{t_{N_2}} \tag{12}$$

where $\mathbf{I}$ is the object's inertia tensor expressed in the inertial frame, time instant $t_{N_1}$ is the time the impulse starts to act and time instant $t_{N_2}$ the time the impulse ends.

To estimate the object's inertia tensor, (12) must contain inertia tensor quantities that remain constant over time. Hence, the tensor $\mathbf{I}$ is expressed in the observation frame, i.e. as ${}^b\mathbf{I}$,

$$\mathbf{R}_{b_{|t_{N_1}}}\,{}^b\mathbf{I}\,{}^b\boldsymbol{\omega}\big|_{t_{N_1}} + \int_{t_{N_1}}^{t_{N_2}} (\mathbf{r}_f \times \mathbf{F}_{contact})dt = \mathbf{R}_{b_{|t_{N_2}}}\,{}^b\mathbf{I}\,{}^b\boldsymbol{\omega}\big|_{t_{N_2}} \tag{13}$$

where ${}^b\mathbf{I}$ is,

$${}^b\mathbf{I} = \begin{bmatrix} I_{xx} & I_{xy} & I_{xz} \\ I_{xy} & I_{yy} & I_{yz} \\ I_{xz} & I_{yz} & I_{zz} \end{bmatrix} \tag{14}$$

Equation (14) can be written in a more convenient form for the estimation procedure as,

$$\mathbf{R}_{b_{|t_{N_1}}}\,{}^b\widehat{\boldsymbol{\omega}}\big|_{t_{N_1}}\,{}^b\widehat{\mathbf{I}} + \int_{t_{N_1}}^{t_{N_2}} (\mathbf{r}_f \times \mathbf{F}_{contact})dt = \mathbf{R}_{b_{|t_{N_2}}}\,{}^b\widehat{\boldsymbol{\omega}}\big|_{t_{N_2}}\,{}^b\widehat{\mathbf{I}} \tag{15}$$

where,

$$\widehat{\boldsymbol{\omega}} = \begin{bmatrix} \omega_x & \omega_y & \omega_z & 0 & 0 & 0 \\ 0 & \omega_x & 0 & \omega_y & \omega_z & 0 \\ 0 & 0 & \omega_x & 0 & \omega_y & \omega_z \end{bmatrix} \tag{16}$$

and

$$\widehat{\mathbf{I}} = \begin{bmatrix} I_{xx} & I_{xy} & I_{xz} & I_{yy} & I_{yz} & I_{zz} \end{bmatrix}^{\mathrm{T}} \tag{17}$$

Using $N_1$ object's attitude measurements at time instants $t_1, t_2, ..., t_{N_1}$ before the impulse application and $N_2$ object's attitude measurements at time instants $t_{N_2}, t_{N_2+1}, ..., t_{N_3}$ after the impulse application, and using the force measurements generated by the force sensor during the time interval $[t_{N_1}, t_{N_2}]$, i.e. the time duration of contact, the following system of equations results

$$\begin{gathered}
\mathbf{R}_{b_{|t_1}}\,{}^b\widehat{\boldsymbol{\omega}}\big|_{t_1}\,{}^b\widehat{\mathbf{I}} = \mathbf{R}_{b_{|t_2}}\,{}^b\widehat{\boldsymbol{\omega}}\big|_{t_2}\,{}^b\widehat{\mathbf{I}} \\
\ldots \\
\mathbf{R}_{b_{|t_{N_1-1}}}\,{}^b\widehat{\boldsymbol{\omega}}\big|_{t_{N_1-1}}\,{}^b\widehat{\mathbf{I}} = \mathbf{R}_{b_{|t_{N_1}}}\,{}^b\widehat{\boldsymbol{\omega}}\big|_{t_{N_1}}\,{}^b\widehat{\mathbf{I}} \\
\mathbf{R}_{b_{|t_{N_1}}}\,{}^b\widehat{\boldsymbol{\omega}}\big|_{t_{N_1}}\,{}^b\widehat{\mathbf{I}} + \int_{t_{N_1}}^{t_{N_2}} (\mathbf{r}_f \times \mathbf{F}_{contact})dt = \mathbf{R}_{b_{|t_{N_2}}}\,{}^b\widehat{\boldsymbol{\omega}}\big|_{t_{N_2}}\,{}^b\widehat{\mathbf{I}} \\
\mathbf{R}_{b_{|t_{N_2}}}\,{}^b\widehat{\boldsymbol{\omega}}\big|_{t_{N_2}}\,{}^b\widehat{\mathbf{I}} = \mathbf{R}_{b_{|t_{N_2+1}}}\,{}^b\widehat{\boldsymbol{\omega}}\big|_{t_{N_2+1}}\,{}^b\widehat{\mathbf{I}} \\
\ldots \\
\mathbf{R}_{b_{|t_{N_3-1}}}\,{}^b\widehat{\boldsymbol{\omega}}\big|_{t_{N_3-1}}\,{}^b\widehat{\mathbf{I}} = \mathbf{R}_{b_{|t_{N_3}}}\,{}^b\widehat{\boldsymbol{\omega}}\big|_{t_{N_3}}\,{}^b\widehat{\mathbf{I}}
\end{gathered}$$

This system of equations can be written in a matrix form,

$$\mathbf{A}\,{}^b\widehat{\mathbf{I}} = \mathbf{b} \tag{18}$$

where $\mathbf{A}$ and $\mathbf{b}$ are given by

$$\mathbf{A} = \begin{bmatrix}
\mathbf{R}_{b_{|t_2}}\,{}^b\widehat{\boldsymbol{\omega}}\big|_{t_2} - \mathbf{R}_{b_{|t_1}}\,{}^b\widehat{\boldsymbol{\omega}}\big|_{t_1} \\
\ldots \\
\mathbf{R}_{b_{|t_{N_1}}}\,{}^b\widehat{\boldsymbol{\omega}}\big|_{t_{N_1}} - \mathbf{R}_{b_{|t_{N_1-1}}}\,{}^b\widehat{\boldsymbol{\omega}}\big|_{t_{N_1-1}} \\
\mathbf{R}_{b_{|t_{N_2}}}\,{}^b\widehat{\boldsymbol{\omega}}\big|_{t_{N_2}} - \mathbf{R}_{b_{|t_{N_1}}}\,{}^b\widehat{\boldsymbol{\omega}}\big|_{t_{N_1}} \\
\mathbf{R}_{b_{|t_{N_2+1}}}\,{}^b\widehat{\boldsymbol{\omega}}\big|_{t_{N_2+1}} - \mathbf{R}_{b_{|t_{N_2}}}\,{}^b\widehat{\boldsymbol{\omega}}\big|_{t_{N_2}} \\
\ldots \\
\mathbf{R}_{b_{|t_{N_3}}}\,{}^b\widehat{\boldsymbol{\omega}}\big|_{t_{N_3}} - \mathbf{R}_{b_{|t_{N_3-1}}}\,{}^b\widehat{\boldsymbol{\omega}}\big|_{t_{N_3-1}}
\end{bmatrix} \tag{19}$$

$$b = \begin{bmatrix} \mathbf{0}_{3x1} \\ \cdots \\ \mathbf{0}_{3x1} \\ \int_{t_{N_1}}^{t_{N_2}} (\mathbf{r}_f \times \mathbf{F}_{contact}) dt \\ \mathbf{0}_{3x1} \\ \cdots \\ \mathbf{0}_{3x1} \end{bmatrix} \quad (20)$$

To solve for ${}^b\hat{\mathbf{I}}$, at least one measurement before or after impulse is required and necessarily the measurements during the time interval $[t_{N_1}, t_{N_2}]$. The system in (18) is over-determined and it is solved using least-squares as,

$${}^b\hat{\mathbf{I}} = (\mathbf{A}^T\mathbf{A})^{-1}\mathbf{A}^T\mathbf{b} \quad (21)$$

## 3 SIMULATION STUDY

For the simulation study an appropriate model in MSC Adams was created. Specifically, the model consists of a chaser system with a rod mounted on it, and a target object, see Fig. 5. The chaser system is a metal cylinder of radius 0.6 m and length 2 m. The rod is a metal cylinder of radius 0.025 m and length 1.5 m. The target is a 2x1x1 $m^3$ box. The observation frame of the target has the same orientation as the principal axes, without loss of generality. The target is set to be rotated freely with angular velocity $\boldsymbol{\omega} = \begin{bmatrix} 5 & 5 & 30 \end{bmatrix}^T$ deg/s and to be translated with a velocity $\mathbf{v}_{cm} = \begin{bmatrix} 0.05 & 0.06 & 0.07 \end{bmatrix}^T$ m/s.

The parameters of the contact model selected are presented in Tab. 1. The step size of the simulation is 0.1 ms and the simulation duration is 4 s. The identification results are presented in Tab. 2. As shown in this table, the proposed method estimates all the inertia parameters of the space object successfully.

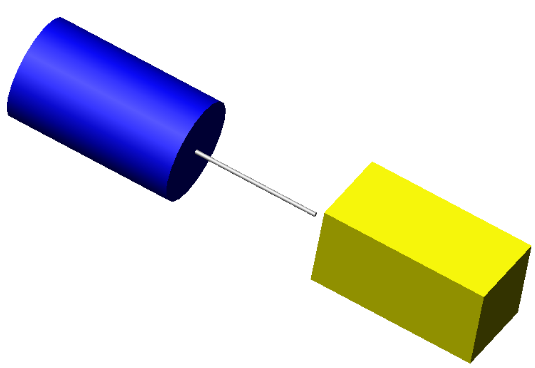

*Figure 5: Simulated model in MSC Adams.*

Table 1. Contact Model Parameters.

| | |
|---|---|
| Contact Type | Solid to Solid |
| Normal Force | Impact |
| Stiffness | $10^8$ N/m |
| Force Exponent | 1.1 |
| Damping | $10^4$ Ns/m |
| Penetration Depth | 0.0001 m |

Table 2. Simulation Results.

| Para-meters (SI units) | True Value | Estimated Value | Relative Error (%) |
|---|---|---|---|
| $M$ | 5480 | 5663.2 | -3.34 |
| ${}^b r_{0_x}$ | 0.5 | 0.4998 | 0.04 |
| ${}^b r_{0_y}$ | -0.1 | -0.1 | 0 |
| ${}^b r_{0_z}$ | 0.19 | 0.1892 | 0.42 |
| $I_{xx}$ | 2283.34 | 2299.0 | -0.6858 |
| $I_{xy}$ | 0 | -2.6 | - |
| $I_{xz}$ | 0 | 0.6 | - |
| $I_{yy}$ | 2283.34 | 2306.3 | -1.0 |
| $I_{yz}$ | 0 | -0.4 | - |
| $I_{zz}$ | 913.34 | 916.4 | -0.3350 |

## 4 EXPERIMENTAL STUDY

The experimental validation of the proposed identification method exploits the Robotic Space Emulator System of NTUA's Control Systems Lab, [12]. In the experimental procedure of this work, the involved parts of the space emulator are the autonomous robot "Cepheus" and a passive object, that are floating over a granite table, see Fig. 6. The granite table has very low surface roughness and very small inclination, thus allowing the development of frictionless microgravity conditions in three dimensions. In this experiment, a rod is mounted on the "Cepheus" robot in order to apply an impulse to the target.

In this section, the experimental identification of the floating passive object is presented. In the first step, a force and moment impulse is given manually to the target object in order to represent a tumbling object in space and subsequently the object is translating and rotating freely. While the object is free-floating, the eight-camera PhaseSpace System of the Space Emulator tracks its motion at 500 Hz. The "Cepheus" robot approaches the target and its rod touches slightly the target. The force sensor mounted at the end of the rod measures the force acting on the chaser robot during their contact. After the application of this impulse, the PhaseSpace System tracks the change of passive object's motion.

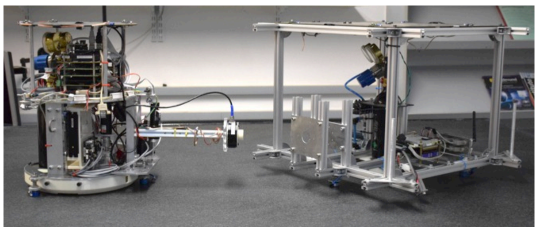

*Figure 6: Chaser Robot* "Cepheus" *(left) and Target Object (right) of NTUA Space Emulator System.*

The position of both the robot and the target are tracked continuously by the PhaseSpace system while the force on the target is derived from force sensor measurements. The feature point of the target is its geometrical center and the feature point of the chaser robot is the geometrical center of its base. The position of these points is tracked during the experiment. Furthermore an observation frame is attached to the target with origin at its feature point while another body-fixed frame is attached to the chaser with origin at its feature point respectively, see Fig. 7.

The measurements required are the position, the velocity, the attitude and the angular velocity of the robot and the target, as well as the force.

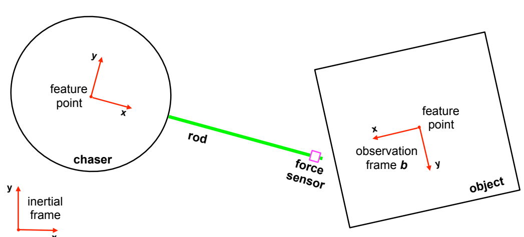


*Figure 7: Feature points and frames of chaser and target.*

To mitigate the measurement noise effect as much as possible, appropriate signal processing is employed. Firstly, the position of the target is differentiated and the obtained velocity measurements are filtered by a third order Butterworth low-pass filter with cutoff frequency at 5 Hz. The angular velocity of the target before and after the impulse is calculated by the slope of the angle with respect to time before and after the impulse, avoiding the amplification of noise effects due to differentiation.

The forces measured by the force sensor were filtered by a third order Butterworth low-pass filter with cutoff frequency at 18 Hz. The appropriate selection of the cutoff frequencies was based on the Fourier transforms of the signals to be filtered. In the case of force filtering, additional insight was provided by the contact frequencies. In addition the force measurements were represented at the force sensor's frame and were expressed in the inertial frame by appropriate transformations. Finally, the forces applied to the target are the opposite of those applied on the chaser expressed in the inertial frame.

The target's velocity and attitude before and after the impulse were fitted by a linear function (first degree polynomial) using the Curve Fitting Toolbox (MathWorks Inc.). Insight about the fit models, i.e. linear functions, was provided by the simulation of the free-floating target based on CAD parameters. In particular, it was observed that in 2D motion, the velocity of the feature point and the attitude of the observation frame are linear functions of time under the condition of free-floating bodies. The decision, on the one hand to fit the velocity and the attitude signals and on the other hand to obtain insight about the fit models from the simulated target based on CAD parameters, was critical for the successful parameter identification.

The time histories of the measured target's velocity, attitude and the derived angular velocity are shown in Fig. 8 and Fig. 9. Based on the measurements of these figures before or after the contact, i.e. when the target is free-floating, the CoM is estimated using (5). It is worth pointing out that the impulse duration in Fig. 8 seems greater that the real one, i.e. 0.03 s, shown in Fig. 9 and Fig. 10. This difference was due to filtering and the specific selection of the cutoff frequency, but that was not an issue for the identification procedure.

Furthermore, the time histories of forces applied on the target are shown in Fig. 10. In this figure it is observed that the contact force mainly lies along the y-axis. Based on the measurements shown in Fig. 8 and Fig. 9, the velocity of the target CoM before and after the contact is estimated by (5). Thus, the target mass is estimated using (9).

To estimate the target's moments of inertia, the measurements of target's attitude and the derived angular velocity, see Fig. 9, are required. In addition, the moment impulse applied on the target has to be measured. The force sensor measurements were transformed in order to be expressed in the inertial frame; their opposite were applied on the target. The forces on the target are shown in Fig. 10.

The point of force application was also estimated. In particular, the position of the feature point on chaser during the contact was $\boldsymbol{r}_{GPS} = [\ 0.83 \quad 1.6\ ]^{\mathrm{T}}$, the vector from chaser's feature point to the end of the rod was known from CAD in chaser's frame and it was transformed to be expressed in the inertial frame, $\boldsymbol{r}_{rod} = [\ -0.03 \quad -0.43\ ]^{\mathrm{T}}$. For this transformation, the chaser attitude during contact, was considered, i.e. -96.24 deg. The position of the target's CoM was calculated using (11), as $\boldsymbol{r}_{cm} = [\ 0.86 \quad 0.89\ ]^{\mathrm{T}}$. In fact, this vector coincides with the position vector of the target's feature point since the target CoM was estimated to be located at target geometrical center. Hence, by (10) the vector from the target CoM to the point of impulse application expressed in the inertial frame is $\boldsymbol{r}_{f} = [\ -0.07 \quad 0.29\ ]^{\mathrm{T}}$.

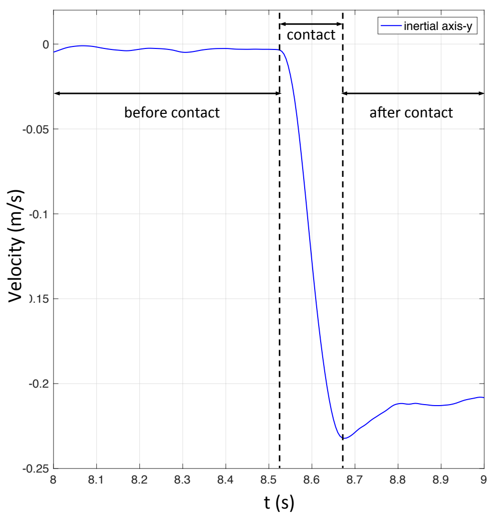


*Figure 8: Measured target's velocity in y-axis with respect to time.*

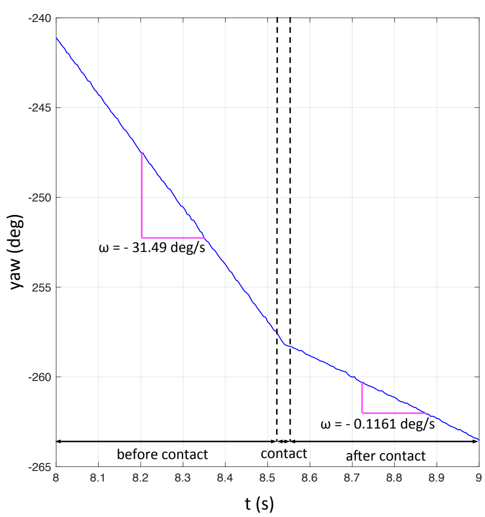


*Figure 9: Measured target's attitude with respect to time.*

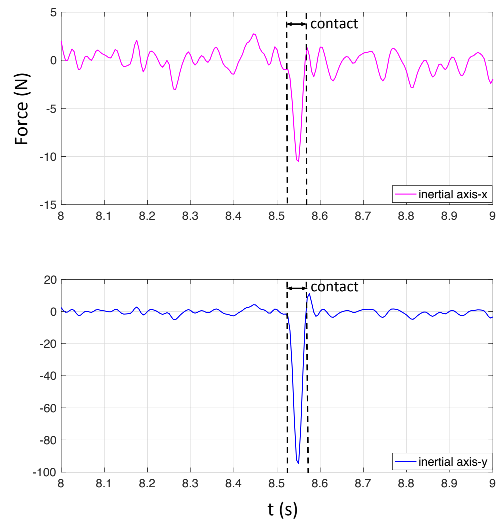


*Figure 10: Measured forces applied to the target with respect to time.*

The identification results are presented in Tab. 3. As shown in this table, the proposed method estimates all the inertia parameters of the space object successfully.

Table 3. Experimental Results.

| Parameters | True Value | Estimated Value | Relative Error (%) |
|---|---|---|---|
| $M$ (kg) | 9.6 | 9.37 | 2.41 |
| ${}^{b}r_{0_x}$ (m) | 0 | 0 | - |
| ${}^{b}r_{0_y}$ (m) | 0 | 0 | - |
| $I_{zz}$ (kg m$^2$) | 0.516 | 0.52 | -0.81 |

## 5 CONCLUSION

In this paper, a method for identifying the full set of inertial parameters of a space object is presented, which is applicable in the pre-capture phase. Using data from visual sensors, the object's CoM and the velocity of the CoM is estimated. In addition, an impulse is applied on the target object by a rod mounted on the chaser system, and by using data by visual and force sensors mounted on the chaser system too, the object's mass and moments of inertia are estimated. The method is based on kinematic and impulse equation. No information about accelerations, which contain substantial noise, is required. The proposed method is validated by a numerical simulation and subsequently it is used for the experimental identification of a floating passive object, part of the NTUA Space Emulator System.

## Acknowledgement

Olga Orsalia Christidi Loumpasefski is supported by an Onassis Foundation Scholarship.

## References

[1] Flores-Abad A, Ma O, Pham K and Ulrich S (2014) A review of space robotics technologies for on-orbit servicing. *Progress in Aerospace Sciences* 68:1-26.

[2] Murotsu Y, Senda K, Ozaki M and Tsujio S (1994) Parametre Identification of unknown Object Handled by Free-Flying Space Robot. *AIAA Journal of Guidance, Control and Dynamics* 17(3):488-494.

[3] Ma O and Dang H (2008) On-Orbit Identification of Inertia Properties of Spacecraft Using a Robotic Arm. *AIAA Journal of Guidance, Control and Dynamics* 31(6):1761-1771.

[4] Xu W, Hu Z, Zhang Y, Wang Z. and Wu X (2015) A practical and Effective Method for Identifying the Complete Inertia Parameters of Space Robots. In: *proceedings of 2015 IEEE/RSJ international conference on intelligent robots and systems (IROS)*, Hamburg, Germany, pp. 5435-5440.

[5] Christidi-Loumpasefski OO, Nanos K and Papadopoulos E (2017) On Parameter Estimation of Space Manipulator Systems Using the Angular Momentum Conservation. In: *proceedings of 2015 IEEE international conference robotics and automation (ICRA)*, Singapore, pp. 5453-5458.

[6] Lichter MD and Dubowsky S (2004) State, shape, and parameter estimation of space objects from range images. In: *proceedings of 2015 IEEE international conference robotics and automation (ICRA)*, New Orleans, USA, pp.2974-2979.

[7] Hillenbrand U and Lampariello R (2005) Motion and parameter estimation of a free-floating space object from range data for motion prediction. In: *proceedings of 2005 international symposium on artificial intelligence, robotics and automation in space (i-sairas)*, Munich, Germany.

[8] Aghili F (2012) A prediction and motion-planning scheme for visually guided robotic capturing of free-floating tumbling objects with uncertain dynamics. *IEEE Transactions on Robotics* 28(3):634-649.

[9] Sheinfeld D and Rock S (2009) Rigid body inertia estimation with applications to the capture of a tumbling satellite. In: *proceedings of 2009 AAS/AIAA space flight mechanics meeting*, Savannah, Georgia.

[10] Meng Q, Liang J and Ma O (2018) Estimate of All the Inertia Parameters of a Free-Floating Space Manipulator System. In: *proceedings of 2018 AIAA guidance, navigation and control conference,* Kissimmee, Florida.

[11] Hughes P (1986) *Spacecraft Attitude Dynamics*, Willey, New York.

[12] Christidi-Loumpasefski OO, Ntinos C and Papadopoulos E (2017) Analytical and Experimental Parameter Estimation for Free-Floating Space Manipulator Systems In: *proceedings of 2017 Symposium on Advanced Space Technologies in Robotics and Automation (ASTRA)*, Leiden, The Netherlands.